ARKIV FÖR FYSIK Band 17 nr 29

Communicated 27 January 1960 by M. Siegbahn

The high-frequency deflection method for measuring short half-lives

Part II. The electron coincidence spectrometer and related arrangements used in connection with the high frequency deflection, time measuring instrument

By Torsten Alväger

With 9 figures in the text

ABSTRACT

The focusing arrangements used in the experimental set-up for investigation of the high frequency deflection method for measuring short half-lives (of the order of 10^{-10} s or less) of isomeric states in nuclei are discussed. This includes a description of an electron-electron coincidence spectrometer. Further the time spread in the analyzing magnets of this is considered. At present this time spread is about 10^{-10} s, but can be decreased considerably, probably by a factor of 10, by a special design of the high frequency deflection system. Some other arrangements, such as a special electrostatic system, which will increase the coincidence counting rate by about an order of magnitude and decrease the time spread, are also discussed.

I. Introduction

The high frequency deflection method is a new way of measuring very short half-lives (of the order of 10^{-10} s or less) of isomeric states in nuclei. The principles of this and a few measurements carried out with the method has recently been described (Part I [1]). The following is a continuation of that description taking into account some of the electron optical arrangements used. A third paper will discuss some other electronic systems as the high frequency arrangement. (Part III [6].)

The principles of the method can best be demonstrated by referring to Fig. 1. S is a sample which is assumed to emit two electrons e_1 and e_2 in cascade and the purpose is to measure the time between these two events. The electrons are focused by the magnets M_1 and M_2 and registered by the scintillation detectors D_1 and D_2 respectively. D_1 and D_2 are coupled in coincidence. This set-up corresponds to a conventional electron-electron coincidence spectrometer in which the time measuring unit is the detectors themselves. With such an arrangement it is sometimes possible to obtain a resolution of the coincidence curve, as defined from the half width, of about 10^{-9} s. However, by inserting two pairs of deflection plates C_1 and C_2, on which a high frequency voltage can be switched on, it is possible to deflect the electron beam passing them and thus pulse the beam reaching the detectors. Thereby one obtains a time sensitive unit, which, if the

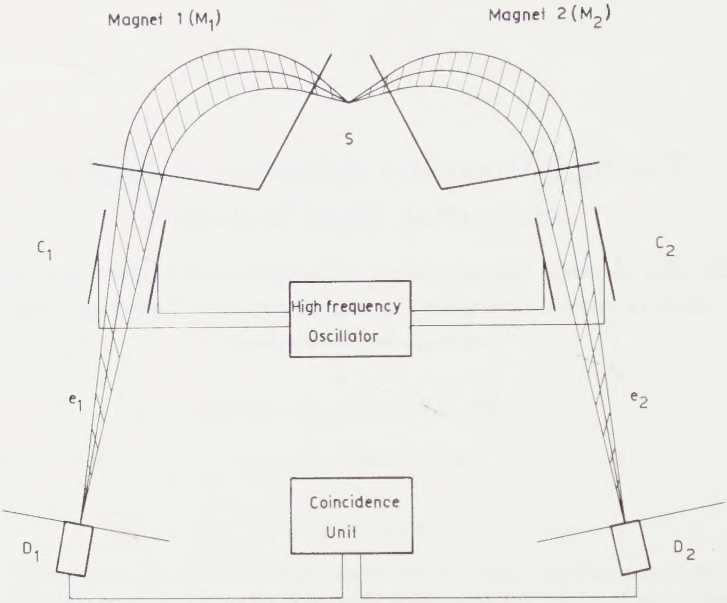

Fig. 1. Diagram of the principle of the high-frequency deflection method. $C_{1,2}$ represent the high frequency deflection plates, $e_{1,2}$ electron trajectories, while $D_{1,2}$ symbolize the detectors.

frequency is chosen high enough, can measure shorter time intervals than what is possible with the detectors alone.

The coincidence resolution curve can be measured in the following way. If the electrons e_1 and e_2 start at the same time from S and if the phase difference between the two voltages at C_1 and C_2 has such a value that it corresponds to the time difference of passage of the electrons e_1 and e_2 through the magnets one observes a coincidence between those electrons which pass the plates without deflection. If, however, for example, the electrons e_2 are delayed, these will be deflected at C_2 by a certain angle with respect to the electrons e_1, which still reached the detector D_1 without deflection. Thus, by moving the detector D_2 or by changing the phase difference between the voltages of the deflecting plates and measuring the corresponding coincidence counting rate, one obtains a coincidence resolution curve. From this it is then possible to estimate the delay of the electrons e_2 in the same way as is used in the conventional delayed coincidence technique.

It has been shown in [1] that it is possible with the method described above and with a relatively simple experimental set-up to obtain a resolving time 2τ of about 3×10^{-10} s and a slope of the coincidence curve which corresponds to a half-life of about 3×10^{-11} s. It is also shown there that the method is suitable for transitions which can be reached from measurements of coincidences between $e^- - e^-, \beta^\pm - e^-$ or $A - e^-$ where $e^-, \beta^\pm$ and A represent conversion, β and Auger electrons, respectively.

The coincidence resolution curve is a function of many variables such as the resolution of the magnetic spectrometers, frequency and voltages of the high frequency system, instabilities etc. For the resolution time mentioned above i.e.

3×10^{-10} s, the energy of the electrons e_1 and e_2 was about 300 and 100 keV, respectively. The resolution of the magnets was set to 0.4 %, while the frequency used was 146 Mc/s which corresponds to a half period time of 3.5×10^{-9} s. The high frequency voltage was a few kV. A further increase of the time resolution can in principle be obtained by an increase of the spectrometer resolution and by using a larger deflection voltage or frequency. If one increase the first two parameters, the coincidence counting rate decreases, which is not the case if one increase the frequency. This is therefore to be preferred. In this way it should be possible to reach a resolution which is at least a factor of 10 or even 100 larger than that now obtained.

The following will describe some of the details used in the experimental set up to investigate the high frequency deflection method. This includes a discussion of the coincidence spectrometer. Further, the time spread of the electrons in the magnets is considered as this sets a limit to the time resolution possible with the present experimental set-up. Another difficulty which is considered is the low intensity. This can be improved in many ways. Here a special system is discussed which should in principle make it possible to get an order of magnitude higher in the coincidence counting rate than now obtainable. This system should also make it possible to decrease the time-spread in the magnets.

2. The coincidence spectrometer

2.1. *General*

The two magnets M_1 and M_2 in Fig. 1 are of a double focusing type and placed at right angles to each other, i.e. coincidences are measured between electrons, which are emitted at 90° to each other. Both magnets can therefore see the same surface of the sample. The usual arrangement in coincidence instruments, where the two focusing arrangements look at different sides of the source, is not used in order to avoid the line broadening from electrons which must pass through the backing of the sample. The set-up used makes it therefore easier to prepare samples. Further, to make it possible for both magnets to see the sample, which usually has an extension of about 2×1 mm^2, the surface of this has to make an angle of about 45° to the surface of the entrance of the magnets. These therefore look at a smaller object than the real geometrical extension of the sample. This means a small increase in the resolution as compared to the case when the sample surface is parallel to the entrance surface of the magnets, because the focus is not sensitive to a small variation in the distance from the sample to the magnets. This fact ought to be exploited more than has been done up to now. As will be seen later (3.1.), due to the large asymmetry of the focusing of the magnets, one has a magnification of the source, which contributes considerably to the line width at the focus. By using a larger angle than 45°, it should be possible to decrease this influence of the sample area of the resolution.

The drawback with the 90° arrangement is that it is impossible to decrease the distance between the sample and the magnets more than to a certain value determined by the dimensions of the magnets. This minimum value is about 5 cm. (The mean radius of the magnets is 15 cm.) A smaller distance would make it possible to use a larger transmission. If the two magnets had been set up at 180° to each other i.e. that one would measure coincidences between electrons going out at an angle of 180° to each other, the sample distance could have been smaller. This would thereby result in an increase in the transmission of about 25 % in comparison with that now used, which is about 0.1 %. However, from practical points of view, the arrangement of the high frequency system being one of these, the 180° set up was not preferable. This fact and the advantage of having the possibilities of using relatively thick backing of the sample, are therefore reasons carrying most weight towards the decision of using the arrangement shown.

The advantage of having a two direction or double focusing field in the present arrangement is not only that it permits relatively large transmission and the use of a small detector in the z- or axial direction i.e. a direction perpendicular to the focusing plan in Fig. 1. There is also the possibility of arranging the h.f.-deflection field so that one can sweep the electron beam in the z-direction, which usually is to be preferred instead of sweeping in the radial direction as discussed in Fig. 1. In this way one can avoid a contamination between electron lines which are not well resolved. If, for example, coincidence measurements are to be made between a β-spectrum or Auger electrons and a conversion electron line, sweeping of the β-beam in the radial direction would make the measurement rather difficult, but the same in z-direction is quite reliable. Further, by utilizing the focusing in the z-direction and thus sweeping the electrons in this direction, one can tolerate a large extension of the slit in the r-direction at the detector. The slit can often be made larger than the line width. Small instabilities in the magnetic field, which move the image mainly in the r-direction, can thus be tolerated without disturbing the time measurements.

2.2. *The magnets*

The magnetic field of a double-focusing spectrometer can be described by the z-component of the field in the symmetry plane $z = 0$ by

$$H_z(r, 0) = H_0(1 - \alpha\varrho + \beta\varrho^2 + \cdots) \tag{1}$$

where $\varrho = \frac{r - r_0}{r_0}$ and α is a constant equal 0.5. The constant β can be chosen in different ways. For a value of $\beta = 0.25$, the field (1) can be realized by using a conical pole surface, [2] which of course has advantages from the constructional point of view. The two analyzing magnets M_1 and M_2 are designed according to this.

The pole distance $2z$ as a function of r can in the case $\beta = 0.25$ be expressed by $2z = \frac{z_0(r + r_0)}{r_0}$, where $2z_0$ is the pole distance at the radius $r = r_0$. In order to have easily handled magnets, the radius r_0 should not be too large: a suitable value being $r_0 = 15$ cm. Other reasons too, for example, the time spread of the electrons passing the magnets (see later) indicated a relatively small value of r_0. For $r_0 = 15$ cm this time spread can be tolerable in many cases. The mean pole distance $2z_0$ is 4 cm. In order to make use to the full of the special advantage of the chosen double focusing field, one should have the radial and axial dimensions of the pole gap of about equal magnitude. However, this should mean a relatively large extension of the magnet in the radial direction in order to

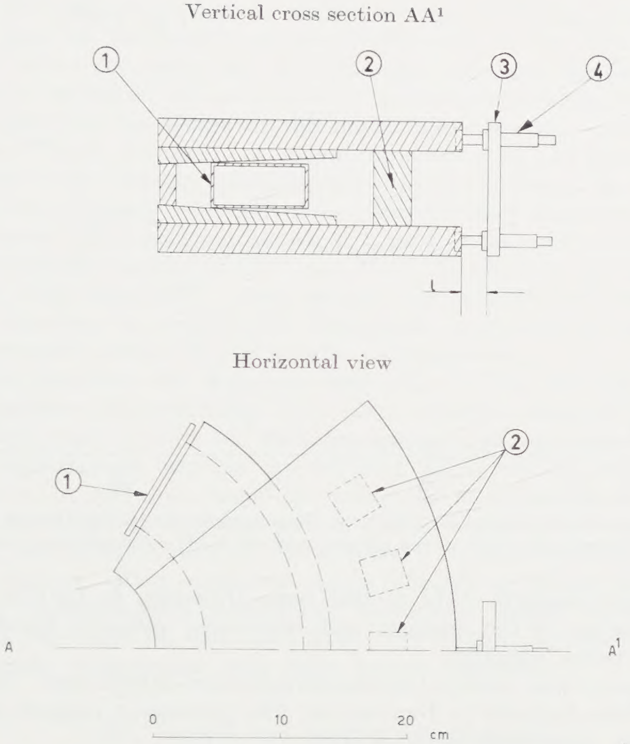
Vertical cross section AA¹

Horizontal view

Fig. 2. Vertical and horizontal section of the analyzing magnets M_1 and M_2. 1 is the vacuum chamber, 2 the permanent magnetic steel pieces, 3 the short-circuiting iron rod and 4 the fine regulation mechanism of this rod.

avoid edge effects. Therefore the smaller value of $2z_0$ has been chosen, even if it implies a decrease of the transmission.

The sector field angle is about 105°, while the distance between the sample and the entrance surface of the magnets is 7.5 cm and the distance between the exit surface and the image is 125 cm. The fringing field makes, however, that these figures change somewhat when the optical properties of the field are taken into account. The distances are then about 2 cm smaller, while the sector field angle increases to about 120°. The purpose of having this very asymmetrical focusing arrangement is two fold: firstly, the distance between sample and magnet must be small to get maximum transmission and, secondly, the distance between image and magnet must be large to have space for the hf deflection plates.

The shape of the magnets can be seen in Fig. 2, which gives a vertical and horizontal section of these.

2.3. *The magnetization of the magnets*

The magnets are built so that they can be excited both with a coil and with permanent magnets. The last mentioned method is usually preferred when the instrument is adjusted for time measurements because of the simplicity of ob-

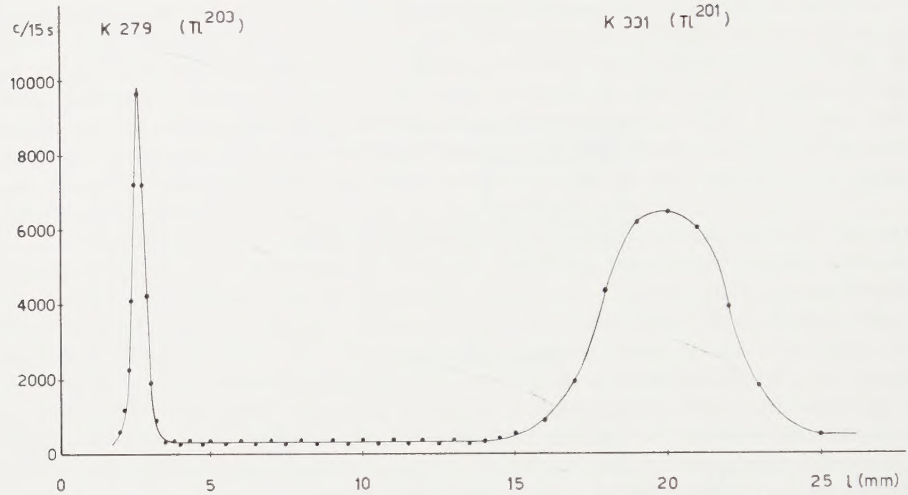

Fig. 3. The shape of two conversion electron lines measured as a function of l i.e. the distance between the yoke of the magnet and the short-circuiting iron rod.

taining a stable magnetic field in this case. However, to be able to investigate focusing properties of the magnets and sometimes unknown spectra, the use of a coil is, of course, superior.

The permanent steel used is the aluminium-nickel-cobolt steel "Fama 700" from the Swedish firm Fagersta in Dannemora. The permanent magnet steel pieces[1] are prismatic with dimensions $3 \times 3 \times 6$ cm^3.

The amount of permanent steel needed can be calculated from the well known relation $A_s l_s = H_g^2 A_g l_g q / H_s B_s$, where A_s, A_g and l_s, l_g are the cross sections and lengths of the steel and the air-gap, respectively, q a leakage factor, H_s the field strength in the steel and H_g the field strength in the air-gap and B_s, finally, the flux density in the permanent magnet steel. In the above relation it is assumed that the loss of magnetic potential in the yoke is negligible and that the field in the air-gap is uniform. For the permanent magnet steel used here $H_s B_s$ has a value of $1.2 \cdot 10^6$.

To obtain a magnetic field in the air-gap of 300 gauss, corresponding to about 1 MeV electrons, when the radius $r_0 = 15$ cm, $A_s l_s$ is approximately $= 162$ cm^3 if the area of the air-gap is 360 cm^2, the pole distance 4 cm and a leakage factor of 1.5 is used. Owing to over simplification of the relation used the actual amount of steel needed is somewhat more than the calculated value but the necessary field is easily obtained with a few pieces of the steel.

The permanent magnet pieces are situated between the yoke of the magnet as seen in Fig. 2 and can be fixed by screws through the yoke.

2.4. *Regulation of the magnetic field*

To make it possible to regulate the field of the magnets continuously when using the permanent magnets, it was found valuable to use the arrangement shown in Fig. 2. It consists simply of a steel plate 3 for which the distance to the yoke of the magnet (l) can be varied between 0–10 cm. The system is so dimensioned that for the range most frequently used one can vary the field about 25 %. This is about the value the field changes when the volume of the permanent magnets is increased by one standard piece. It is obvious that by a regulation of this type the line shape of the image measured as a function of l will vary strongly. This is, however, of minor importance in the present case as the purpose seldom is to measure energies etc. Just to illustrate the line shape as a function of l Fig. 3 shows two conversion electron lines taken up with the fine regulation system. The spectrum shown is a part of that obtained from a sample containing a mixture mainly of Pb^{203} and Pb^{201}. The lines are $K\,279$ in the decay of Pb^{203} and $K\,331$ from Pb^{201}, with energies 193 and 245 keV respectively. The resolution in this case is about 0.5 %. This figure is obtained by comparison with earlier measurements made by use of the coil system.

---

[1] We are very much indebted to Prof. Slätis for putting these at our disposal.

The relation between the magnetic field (H_g) in the focusing part and the distance (l) between the regulating steel plate and the magnetic yoke is not so easily calculated that it can be used for energy determination. But for some purposes an approximate relation can be used which can sometimes be valuable for identification of unknown lines. By using the same process as in the evaluation of the relation giving $A_s l_s$ used above, (in 2.3) one gets the following function connecting H_g and l: $H_g l + a H_g - b l = c$. a, b and c are here functions of the dimensions of the magnet. Often when one has a line-rich spectrum the constants a, b and c can be experimentally determined from some easily found lines. Other unknown lines can then be identified from this. Usually however, lines are identified by intensity comparison with some known spectrum.

2.5. *Sample and detector arrangements*

The sample is fixed in position by a vertical holder, which can be introduced into the spectrometer through a vacuum lock system. This makes it possible to maintain the high vacuum in the main system when changing to a new sample. This is very important as the high frequency deflection system needs a long out-gasing period after it has been exposed to air. This should therefore make it difficult to measure on short-lived activities in absence of a vacuum lock system.

As detectors plastic scintillators are used, which are mounted directly on the photomultipliers. These are of the type RCA 6342. The detectors are coupled in coincidence; the resolution time 2τ of the coincidence equipment used is 3–10 mμs. The crystals have a size of about $25 \times 25 \times 1$ mm^3. The part of the crystal that is exposed to the beam can be varied by an external regulating slit. As the h.f. deflection is made in the z-direction, the extension of the slit in this direction is usually about 5–10 mm, corresponding to about the half width of the beam. By utilizing a smaller opening it would be possible to obtain a larger time resolution for a constant value of the h.f. deflection voltage, but the intensity is usually too small to allow of a small slit width. A suitable compromise between the requirements of the h.f. deflection field and the coincidence counting rate seems to give a slit extension which is about the half width of the beam.

In the radial direction, the maximum extension of the crystals is usually used. This corresponds to an energy resolution of about 2 %. When there is a risk for mixing of neighbouring energies, this opening is, of course, diminished. But when

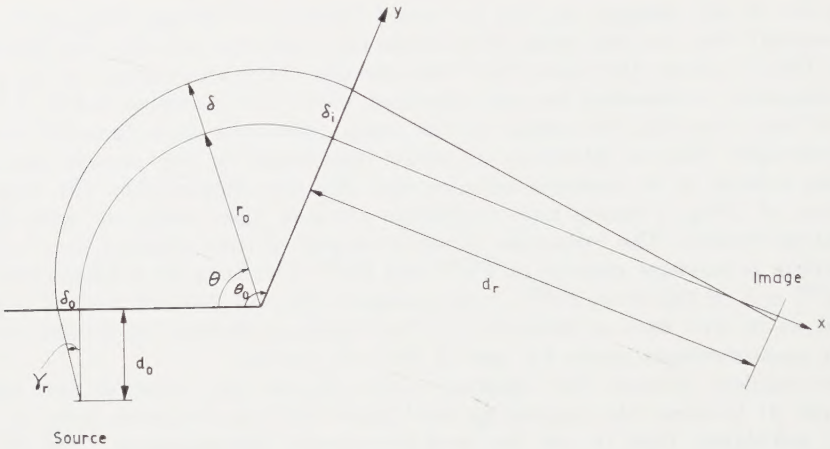

Fig. 4. Definition of some of the symbols used in the text. The z-direction is perpendicular to the plane of the figure.

a single conversion line is focused, it is convenient, as discussed earlier, to have the detector larger than the line breath, as one then can tolerate instabilities of the magnetic field etc. without the time measurements being influenced.

However, there is often a need to have an even larger radial apertures at the detectors than that used. This should make it possible to get higher counting rates in some cases, especially where measurements are performed on β or Auger electrons. From the point of view of the time spread of the electrons in the analyzing magnets, it should be possible to make use of a rather large part of a β-spectrum as discussed below (in 4.2). From the point of view of the high-frequency system, however, a not too large part of the β-spectrum is utilisable. The amount depends upon the magnitude of the half-life measured. For a β-spectrum with maximal energy of say 200 keV at least 10 % of the total β-intensity can often be used. This has also been done in some measurements [1]. In these cases the size of the detector crystals has been too small to make it possible to register the desired amount. Instead of using a larger crystal, which would cause several practical problems, a special focusing magnet placed just infront of the detector has been incorporated. The size and construction of this magnet is equal to that shown in Fig. 2. The field is, however, homogeneous. This magnet not only serves as a unit focusing together for example a large energy continuum to a small spot, but also decreases the background which sometimes is convenient.

2.6. *First order focusing*

The exact position of the image was obtained experimentally by measuring the line width of a certain conversion line as a function of the position of the magnets, while keeping the sample in a fixed position. The focusing optimum was found for a value of d_0 equal about 5 cm and $d_r = d_z = 123$ cm. d_0 represents the distance from the sample to the magnetic field and d_r, d_z the distances from the magnetic field to the image in the radial and axial direction, respectively. See Fig. 4. Both magnets had about the same properties.

It is of interest to compare the experimentally found value for the focusing properties from those general expressions given by, for example, Svartholm [2] and Judd [3]. Introducing the three angles $\phi_{r,z}$, $\phi'_{r,z}$ and $\theta_{r,z}$ where

$$\operatorname{tg} \phi_{r,z} = \frac{d_0}{r_0\sqrt{2}};\ \operatorname{tg} \phi'_{r,z} = \frac{d_{r,z}}{r_0\sqrt{2}};\ \theta_{r,z} = \frac{\theta_0}{\sqrt{2}}$$

and the relation $\phi_{r,z} + \phi'_{r,z} + \theta_{r,z} = \pi$ the distance d_0 can be calculated from d_r, d_z and θ_0. The indices r and z refer to radial and axial focusing, respectively.

In the present case, the geometrical sector angle of the magnets is $\theta = 105°$. The effective angle is, however, larger due to the fringing field at the entrance and exit. Measurements on the trajectories of the electrons at exit show that the fringing field increase the sector angle to $\theta_0 = 120°$. With this value and $r_0 = 15$ cm, $d_r = d_z = 123$ cm one finds $d_0 = 5.7$ cm which is in good agreement with the measured one.

The focusing arrangement was constructed for a transmission of at least 0.2 % in each channel. However, for several reasons the transmission used is less. For example, the time spread of the electrons, which appears as a consequence of a large radial aperture, makes it impossible to use the full opening angle of the magnets. Another limitation is set by the high frequency deflection plates through which only a limited part of the electron beam can be transmitted in order to avoid defocusing effects (caused by the electric fringing field) of the image by deflection. This can, of course, be avoided by using a larger deflection condenser. This is, however, from the point of view of the construction of the high frequency system often not a simple task. This is so because a large condenser at the end of a transmission line means that the latter must be short which thus set a limit to the magnitude of the condenser.

The cross-section of the beam at the exit of the magnets as determind by the magnitude of the condenser is about 3.5×2.0 cm^2. This can be adjusted by a stopper, the regulation of which is situated outside the vacuum chamber. From the value of the cross-section it is possible to calculate the opening angle in the radial ($2\gamma_r$) and axial ($2\gamma_z$) direction. According to the relations (4) and (8) one has, when $\theta_0 = 120°$ and therefore $\cos \theta_0/\sqrt{2}$ can be neglected and $\sin \theta_0/\sqrt{2} \sim 1$, $\delta = r - r_0 = \sqrt{2}\gamma_r r_0$ and $z = \sqrt{2}\gamma_z r_0$. With $2\delta = 3.5$ cm and $2z = 2.0$ cm one gets $\gamma_r = 0.08$ and $\gamma_z = 0.05$. This is in agreement with measurements made at the entrance of the magnets. The solid angle corresponding to $\gamma_r = 0.08$ and $\gamma_z = 0.05$ is about 0.125 % if the entrance aperture is of rectangular shape.

The transmission ordinarily used has been somewhat more than 0.1 %, as obtained from coincidence measurements. This value is in accordance with that obtained from the knowledge of γ_r and γ_z.

3. The line width of radial and axial image

As the time resolution is strongly dependent on the width of the spectrometer line at the detector, it is necessary to consider this in more detail. The line width has to be known with and without the use of the h. f. deflection plates.

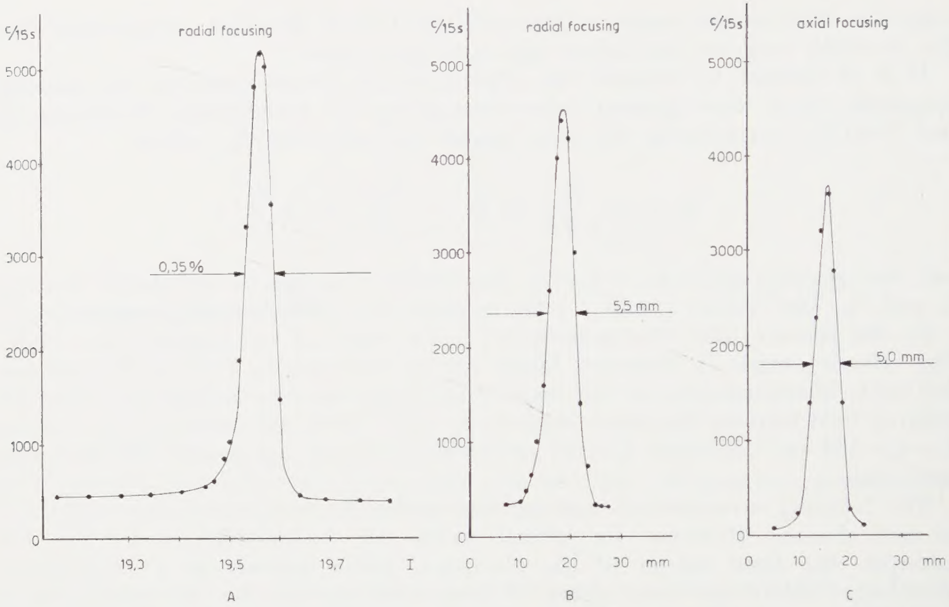

Fig. 5. Resolution and line width for the optimum position of the magnets as measured by the *F* line in ThB (i. e. K 239 in Bi^{212}). A shows the resolution, while B gives the radial extension and C the axial extension of the image.

3.1. *Line width without use of the h.f. deflection plates*

Fig. 5 shows some measurements of resolution and line width made at the focus of the magnets in their optimum position. The electron line used was in all investigations the K conversion electron line of the 239 keV γ-ray from Pb^{212}. This activity was collected on a thin Al-backing, the source area being about 0.5×0.5 mm². In the measurements the radial $(2\gamma_r)$ and axial $(2\gamma_z)$ aperture angles were as large as possible to get maximum transmission. This corresponds thus to $\gamma_r = 0.08$ and $\gamma_z = 0.05$ (2.6). The detector slit area was in all investigations 2.0×20 mm².

Fig. 5 A gives the resolution measured with the coil arrangement. The value obtained in this way was 0.35 %. It should be observed that the high counting rate below the line is due to the β-continuum. The real background can, however. be seen in Fig. 5 C.

Fig. 5 B and C give the absolute dimensions of the images. The radial extension, Fig. 5 B was first measured by moving the detector slit over the line along which the slit extension in the z-direction was larger than the line height. The whole detector arrangement was then turned through 90° and the same procedure was repeated to obtain the axial dimension, Fig. 5 C.

The line width as measured in Fig. 5 is, if one neglects the extension of the measuring slit, mainly due to three effects: the size of the source, the second order aberration of the focusing field and possibly a defocusing effect of the entrance and exit fringing field.

As the focusing arrangement is asymmetrical with $d_0 \ll d_r$, the source size is very important in determining the line width as one gets a large magnification M. According to, for example, Judd [3] M can be written

$$M_{r,z} = \frac{1}{\operatorname{tg} \phi_{r,z} \cdot \sin \theta_{r,z} - \cos \theta_{r,z}} \tag{2}$$

where the indices r and z refer to radial and axial focusing respectively. $\phi_{r,z}$ and $\theta_{r,z}$ are the angles used above (in 2.6). In the present case one has:

$$M = 5.5$$

The error in this figure is about 20 % mainly due to the uncertainty of the trajectories at the entrance and exit of the magnetic field, which make it difficult to estimate the value of d_0 and θ_0 with good precision. In Fig. 5 a large part of the line width is due to the size of the source. Usually, however, it is not possible to prepare sources of the dimensions used in Fig. 5. A normal size is 2×1 mm^2 or even larger. The contribution to the line width from the sample extension is then often even more dominant than in Fig. 5. As mentioned earlier it should be possible, in principle, to decrease this dominance by using a larger angle between the entrance surface of the magnet and the sample surface than that now used which is 45°. It should be pointed out here that in the measurements in Fig. 5 the surface of the sample was parallel to the entrance surface of the magnet.

To obtain an idea of the magnitude of the second order aberration one can calcuate it for an easier but similar case to the present one namely, for a point source and a source distance $d_0 = 0$.

With the notation

$$\varrho = \frac{r - r_0}{r_0}; \ \zeta = \frac{z}{r_0} \tag{3}$$

and with the constants $\alpha = 0.5$ and $\beta = 0.25$ in (1), one can, according to Svartholm [4] write the second order solution for particles in the cylindrical symmetrical field given by (1) as

$$\varrho = \varrho^{(0)} + \varrho^{(1)}; \ \zeta = \zeta^{(0)} + \zeta^{(1)}$$

where

$$\begin{aligned} \varrho^{(0)} &= \sqrt{2} \cdot \gamma_r \cdot \sin \frac{\theta}{\sqrt{2}} \\ \zeta^{(0)} &= \sqrt{2} \cdot \gamma_z \cdot \sin \frac{\theta}{\sqrt{2}} \end{aligned} \tag{4}$$

and

$$\varrho^{(1)} = \left(\frac{\gamma_r^2}{3} - \frac{\gamma_z^2}{6}\right) \left(\cos 2 \frac{\theta}{\sqrt{2}} - \cos \frac{\theta}{\sqrt{2}}\right) \ \frac{\gamma_z^2}{2} \left(1 - \cos \frac{\theta}{\sqrt{2}}\right)$$

$$\zeta^{(1)} = -\frac{2}{3} \gamma_r \gamma_z \left(\cos 2 \frac{\theta}{\sqrt{2}} \ \ \cos \frac{\theta}{\sqrt{2}}\right)$$

γ_r and γ_z are the radial and axial aperture angles defined by shutters.

To define the image position, the coordinate frame shown in Fig. 4 is used. The origin of this system is at the point $r = r_0$, $\theta = \theta_0$. The x-axis is a continuation of the central axis of the spectrometer i.e. it is a tangent to the central axis while the y-axis is in the r-direction at $\theta = \theta_0$.

By using the first order solution one can calculate the location of the image on the x-axis from the boundary condition at the exit. In this way one finds the x-coordinate $x_i = d_{r,z}$ for the image,

$$x_i = -\sqrt{2} \cdot r_0 \cdot \operatorname{tg} \frac{\theta_0}{\sqrt{2}} \tag{5 a}$$

In the same way, the second order solution gives the coordinates y_i and z_i for $x = x_i$

$$\begin{aligned} \frac{y_i}{r_0} = & -\frac{\gamma_r^2}{3}\left[\frac{x_i}{r_0\sqrt{2}}\left(\sin\frac{\theta_0}{\sqrt{2}} + \sin 2\frac{\theta_0}{\sqrt{2}}\right) - \cos\frac{\theta_0}{\sqrt{2}} + \cos 2\frac{\theta_0}{\sqrt{2}}\right] \\ & -\frac{\gamma_z^2}{3}\left[\frac{x_i}{r_0\sqrt{2}}\left(\sin\frac{\theta_0}{\sqrt{2}} + \sin 2\frac{\theta_0}{\sqrt{2}}\right) - \cos\frac{\theta_0}{\sqrt{2}} - \frac{1}{2}\cos 2\frac{\theta_0}{\sqrt{2}} + \frac{3}{2}\right] \end{aligned} \tag{5 b}$$

$$\frac{z_i}{r_0} = -\frac{2}{3}\gamma_r\gamma_z\left[\frac{x_i}{r_0\sqrt{2}}\left(\sin\frac{\theta_0}{\sqrt{2}} - \frac{1}{2}\sin 2\frac{\theta_0}{\sqrt{2}}\right) - \cos\frac{\theta_0}{\sqrt{2}} + \cos 2\frac{\theta_0}{\sqrt{2}}\right]$$

when x_i is large, which corresponds to $\sin \frac{\theta_0}{\sqrt{2}} \sim 1$, (5 b) can be written

$$\begin{aligned} y_i &= -\frac{r_0}{3}\left[\gamma_r^2\left(\frac{x_i}{r_0\sqrt{2}} - 3\right) + \gamma_z^2\frac{x_i}{r_0\sqrt{2}}\right] \\ z_i &= -\frac{2}{3} r_0 \gamma_r \gamma_z \frac{x_i}{r_0\sqrt{2}} \end{aligned} \tag{5 c}$$

with $\gamma_r = 0.08$, $\gamma_z = 0.05$ and x_i/r_0 equal the value used in the present experimental set-up one finds from (5 c)

$$|y_i| \sim 0.15 \text{ cm}$$
$$|z_i| \sim 0.20 \text{ cm}$$

By comparing this value and that due to the magnitude of the source with the experimentally line width shown in Fig. 5 one could state that defocusing effects from the entrance and exit fringing field should be of less importance. This is so because one has also to take into account the finite width of the measuring slit used in the measurements given in Fig. 5. That the fringing field does not give any notable contribution to the line width could be expected as the entrance angle is very small and the electrons at the exit form a nearly parallel beam.

3.2. *Line width with use of the h.f. deflection plates*

When the electron beam is deflected by the h.f. plates one has also to consider the aberration due to these. In the following it is assumed that the deflection is performed in the z-direction and that the h.f. condenser, which consists of two plane parallel plates where the electric field is balanced, is situated at $x = x_d$. If now the electrons are supposed to be focused to a point at $y = 0$; $z = 0$; in the plane $x = x_i$ in the absence of a deflecting field, one can, according to, for example P. A. Sturrock [5] write the coordinates of the deflected spot y_i and z_i at $x = x_i$ as

$$\begin{aligned} y_i &= y_i^{(1)} + y_i^{(3)} \\ z_i &= z_i^{(1)} + z_i^{(3)} \end{aligned} \tag{6}$$

where $y_i^{(1)} = 0$ and $z_i^{(1)} = D_z$. Further,

$$\begin{aligned} y_i^{(3)} &= 2\,P\,D_z\,y_d\,z_d + 2\,R\,D_z^2\,y_d \\ z_i^{(3)} &= P\,D_z\,y_d^2 + 3\,Q\,D_z\,z_d^2 + 2\,S\,D_z^2\,z_d + T\,D_z^3 \end{aligned} \tag{7}$$

In these relations P, Q, R, S and T represent the different aberrations and y_d and z_d the coordinates which give the maximum extension of the beam at $x = x_d$. In the present case, where D_z and the length of the deflection plates p are small in comparison with $(x_i - x_d) = L$, one has $P = L^{-2}$, $Q = 0$, $R = -0.25\,L^{-2}$, $S = -(p\,L)^{-1}$ and $T = \frac{1}{8}\,L^{-3}\,p$. The only term in (7) which has to be taken into account is therefore that containing S, which represents the astigmatism. For $D_z = 5$ cm, $L = 100$ cm, $p = 10$ cm and $z_d = 1.0$ cm one finds $|z_i^{(3)}| = 0.05$ cm, which thus also can be neglected here. This is in accordance with experimental investigations on the arrangement used, which show that no broadening of the image occurs for small values of D_z. The measurements have been performed by studying the line shape of the image after a deflection of the electron beam obtained by applying a D.C. voltage to the high frequency deflection plates. However, in cases where the aberrations, both from the fringing field and the field inside the plates, would be of importance, it seems possible to correct for them to a large degree as is done in many other electron optical instruments.

4. The time spread in the magnets

4.1 *Time spread due to differences in path lengths*

The high frequency deflection plates are placed behind the magnets, mainly because this is the easiest arrangement from a practical point of view. The drawback with the set-up is, however, that electrons following different paths in the magnet will arrive at different times at the exit. This may thus appear as a time spread in the coincidence resolution curve. To get an upper limit of this time spread one can proceed in the following way.

Inside the magnetic field the equation for the trajectory of monoenergetic electrons in the median plan, $z = 0$ is $r - r_0 = a \sin \frac{\theta}{\sqrt{2}} + b \cos \frac{\theta}{\sqrt{2}}$ (cf. e.g. [4]). The constants a and b can be determined from the boundary conditions at the entrance of the field. (See Fig. 4.) One obtains:

$$r - r_0 = \sqrt{2} \cdot r_0 \cdot \gamma_r \sin \frac{\theta}{\sqrt{2}} + d_0 \cdot \gamma_r \cdot \cos \frac{\theta}{\sqrt{2}}, \tag{8}$$

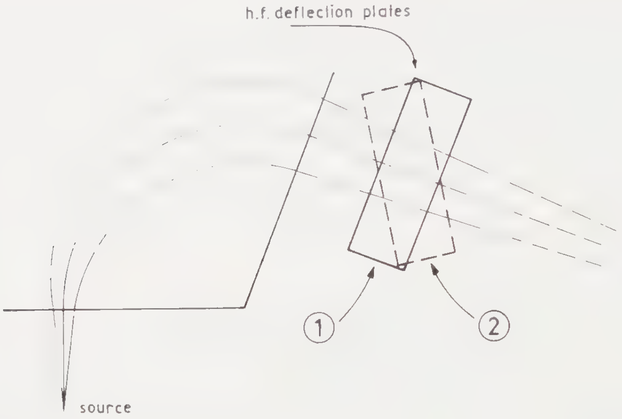

Fig. 6. One example of how it would be possible to correct for the time spread of the electrons caused by the different trajectories in the magnet. With the high frequency (h.f.) deflection plates in position 2 it seems possible to obtain a suitable correction.

where γ_r is the radial aperture angle and d_0 the distance from the source to the magnet.

The path length s inside the field is then approximately, as one can neglect $dr/d\theta$ in comparison with r

$$s=\int_0^{\theta_0} r\,d\theta = r_0\theta_0+\gamma_r\left[2r_0\left(1-\cos\frac{\theta_0}{\sqrt{2}}\right)+\sqrt{2}\cdot d_0\cdot\sin\frac{\theta_0}{\sqrt{2}}\right] \tag{9}$$

The maximum path difference Δs in the radial direction is therefore

$$\Delta s = 2\gamma_r\left[2r_0\left(1-\cos\frac{\theta_0}{\sqrt{2}}\right)+\sqrt{2}\cdot d_0\cdot\sin\frac{\theta_0}{\sqrt{2}}\right] \tag{10}$$

The time spread in the z-direction can, to the first approximation, be neglected. Relation (10) therefore gives the total time spread.

For $r_0 = 15$ cm, $d_0 = 5$ cm, $\gamma_r = 0.075$ and $\theta_0 = 120^\circ$ and an energy of the electrons of 500 keV, corresponding to a velocity of $2.6 \cdot 10^{10}$ cm/sec, one obtains from (10) $\Delta s = 5.1$ cm, and, therefore, a total time spread of about $2 \cdot 10^{-10}\,s$. For lower energies it is often necessary to use a value of γ_r smaller than 0.075 in order to decrease the time spread. It is obvious that this time spread sets a limit to what is possible to measure with the present arrangement. $10^{-10}\,s$ seems to be such a limit of the resolution.

However, there are several ways in which to avoid this hindrance. Still using the same set-up as now, with the high frequency deflection plates behind the magnets, one can arrange the apparatus as shown in Fig. 6 for example. This shows one of the magnets together with one pair the deflection plates. Position 1 of the h.f. plates is that now used. Here all electrons strike the surface of the entrance of the plates roughly to a right angle. However, by turning the deflection system in position 2, which is done by rotating the plates through a certain angle in the horizontal plane, one obtains a correction for the time spread. This

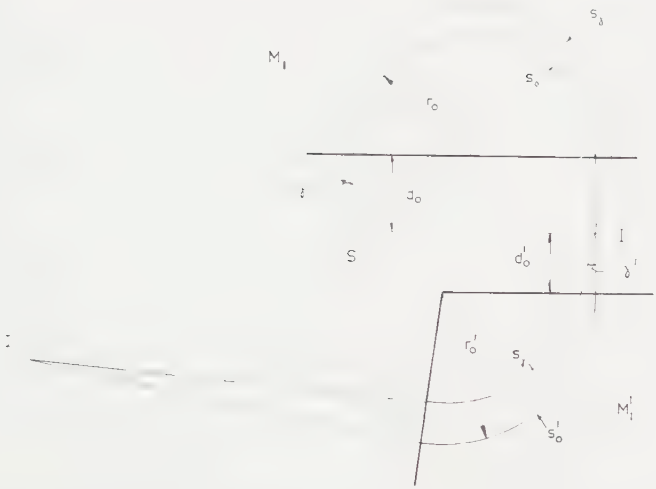

Fig. 7. A time spread correction obtained by use of two magets M_1 and M_1' in each channel of the coincidence spectrometer. The high frequency plates are assumed to be situated behind the magnet M_1'.

is so because the electrons which have traversed the longest distance in the magnet reach the deflection plates first etc. The angle necessary is easily obtained from (10).

Another system which would decrease the time spread is an arrangement consisting of two analyzing magnets in each channel of the coincidence spectrometer. The time spread in the first magnet would then be compensated in the last one. This has been mentioned in [1]. Fig. 7 shows such a system. M_1 and M_1' represent the two magnets. These have the mean radius r_0 and r_0' and deflection angles θ_0 and θ_0', respectively. The electrons from the source S are focused by M_1 to an image I, which then is used as an object for the magnet M_1'. The image of this is I'. The high frequency deflection plates are assumed to be situated just behind the magnet M_1'. s_γ, s_0 etc. represent different paths, where s_γ is a continuation of $s_{\gamma'}'$ etc.

If s_γ, $s_{\gamma'}'$ etc. also represent the length of the trajectories the condition for a compensation of the time spread to the first approximation is now

$$s_\gamma + s_{\gamma'}' = s_0 + s_0'$$

If one assumes for simplicity the two angles γ and γ' in M_1 and M_1' to be equal, one can, according to (9), write the condition given above as:

$$2\,r_0\left(1-\cos\frac{\theta_0}{\sqrt{2}}\right)-\sqrt{2}\cdot d_0\cdot\sin\frac{\theta_0}{\sqrt{2}}=2\,r_0'\left(1-\cos\frac{\theta_0'}{\sqrt{2}}\right)+\sqrt{2}\cdot d_0'\cdot\sin\frac{\theta_0'}{\sqrt{2}},$$

where d_0 and d_0', as usual, are the distances from the sources to the magnets.

The value of θ_0 should be as large as possible to get a small path length. The only restriction is that the source S should be outside the magnetic field. A suitable choice is $\theta_0 = 180^\circ$. The value of θ_0' must be less than θ_0. If one takes $\theta_0' = 120^\circ$, i.e. equal to that now used in the analyzing magnets, one finds if d_0 and d_0' are equal, for example, that the radius r_0 and r_0', too must be of the same magnitude. To get a large deflection sensitivity a small value of d_0' is more practical. If $d_0 \gg d_0'$ one obtains $2 r_0 \sim r_0'$, which seems to be a suitable choice.

Other methods, too, can possibly be used to correct for the time spread, such as a special shaping of the exit of the magnets. The best way seems, however, to be the first mentioned one namely that shown in Fig. 6.

With a correction system one can probably never hope to increase the time resolution more than by a factor of 10 better than now obtainable. Also, it is then necessary to take into consideration the time spread in the axial direction, which in the present arrangement is an order of magnitude smaller than the time spread in the radial direction. To reach extremely short times, the best method is to put the high frequency deflection plates just in front of the magnets. Such a choice means, among other things, that a larger value of d_0 than now must be used in order to get space for the h.f. deflection condensers. Therefore to obtain the same transmission as now one must use larger magnets etc. Further, the deflection sensitivity of the h.f. plates is less in this case by an amount roughly $\frac{L'}{L} M$ as compared with that in the present set-up if the amplitudes of the high frequency voltage are equal in the two cases. L is the distance between the detector and the deflection plates, when these are situated behind the magnets, while L' represents the distance between the sample and the h.f. plates when these are placed in front of the magnets. M is the magnification of the magnets. If the value of M is that now used it is obvious, as L' in all practical cases must be at least a factor of ten less than L, that a larger voltage of the h.f. system is needed in the proposed arrangement to get the same sensitivity as that obtained in the present apparatus. This is, however, no serious objection against the method. To reach a resolution of 10^{-12} s it seems to be the only possible way.

4.2. *Time spread due to differences in energy*

In the analysis above, only monoenergetic electrons have been discussed. Often, however, it is suitable to measure on a part of a β-continuum or a group of Auger electrons. It is then necessary to know the time spread of the electrons in the magnets due to energy differences. Qualitative estimations on the system used show that this time spread is small in comparison with some other types of time spread as that in 4.1. Assume, for example, that an electron group with energy E is focused and that the maximum opening angle of the magnet is used. An electron with a somewhat higher energy $E + \Delta E$, which initially coincided with the central ray will then, of course, follow a certain larger path in the magnet than the central ray. If the energy increase ΔE is so chosen, that it corresponds to the maximum energy which is possible to focus simultaneously with E, then it is obvious that the path for the electron with the energy $E + \Delta E$ is less than the path corresponding to the energy E and maximum opening angle. This means, therefore, a larger time spread in the latter case. Further, electrons with different energies pass indeed the analyzing magnet in different paths, but those with larger path length, corresponding to higher energies, pass with larger velocities. This should, therefore in part compensate for the time spread.

Even if the time spread due to small energy differences thus should be of less importance according to the facts mentioned above it is of interest to have a more quantitative estimation of the effect. This can be obtained by comparing two electrons with velocities v and $v+\Delta v$, respectively, and where the first mentioned electron should follow the ray equation $\delta = r - r_0 = 0$; $z = 0$. If the second electron satisfies the initial condition $\delta(\theta = 0) = 0$ and $d\delta(\theta = 0)/d\theta = 0$ and if $\frac{\Delta v}{v} \ll 1$, the equation for the trajectory of this particle is (cf. e.g. [4])

$$\delta = 2\frac{\Delta v}{v} r_0 \left(1 - \cos\frac{\theta}{\sqrt{2}}\right) \tag{11}$$

The path lenght s in the magnetic field for the electrons with velocity $v+\Delta v$ is now:

$$s_{v+\Delta v} = \int_0^{\theta_0} r\,d\theta = r_0\theta_0 + 2r_0\frac{\Delta v}{v}\left(\theta_0 - \sqrt{2}\sin\frac{\theta_0}{\sqrt{2}}\right) \tag{12}$$

The time necessary to pass this length is

$$t_{v+\Delta v} = \frac{s_{v+\Delta v}}{v+\Delta v} = \frac{r_0\theta_0}{v} + \frac{\Delta v}{v}\frac{r_0}{v}\left(\theta_0 - 2\sqrt{2}\cdot\sin\frac{\theta_0}{\sqrt{2}}\right) \tag{13}$$

and therefore the time spread will be

$$\Delta t = t_v - t_{v+\Delta v} = \frac{r_0}{v}\frac{\Delta v}{v}\left(2\sqrt{2}\cdot\sin\frac{\theta_0}{\sqrt{2}} - \theta_0\right) \tag{14}$$

In the present case $\theta_0 = 120^\circ$ and $r_0 = 15$ cm. Further, by choosing $v = 1.5$ 10^{10} cm/s corresponding to an energy of 79 keV and $\Delta v/v \sim 0.02$, which means an increase in energy of about 5 %, relation (14) gives $\Delta t = 1.5 \times 10^{-11}$ s. To this value one must add the time spread obtained from the electron paths in front of and behind the magnet. This is of the same order of magnitude as the time spread in the field. In all cases, however, the time spread due to small variations in energy of the electrons is negligible in comparison with the time spread caused by the finite value of the opening angle, as shown above.

5. An arrangement to increase the transmission of the spectrometer

The coincidence counting rate is proportional to the product of the transmissions of the two magnets. As this transmission is relatively small, the coincidence measurements are very tedious. An investigation of a suitable metastable state of a nucleus can take several weeks at present. This is of course from, for example, stability point of view, not convenient. By introducing a multichannel system i.e. by using instead of one crystal at D_2 (Fig. 1) several crystals placed parallel in the deflection direction, the measuring time can be reduced considerably: about a factor of 10 as discussed in [1]. However, there are still need for larger transmission in the magnets. This can of course, be obtained just by accepting a larger opening angle of the magnets. But this means larger dimensions of the instrument and increased time spread. With the arrangements described in the

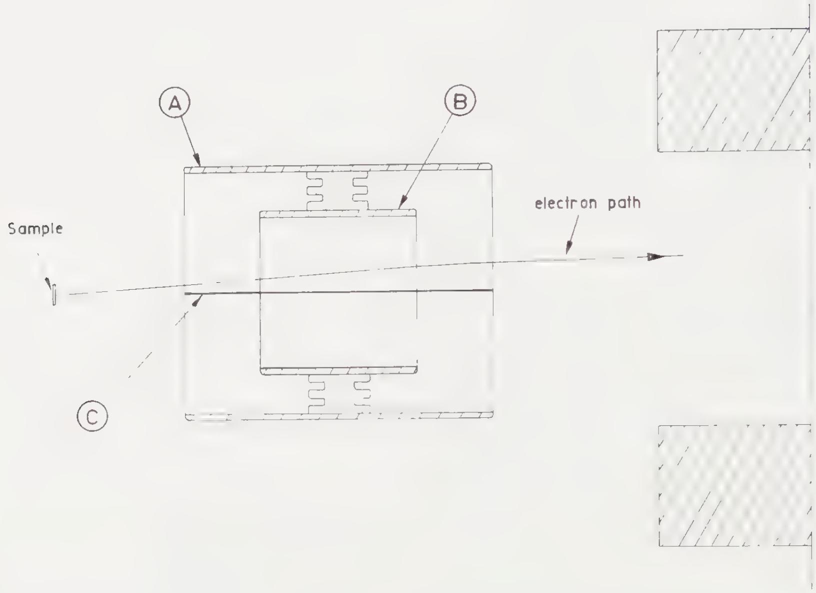

Fig. 8. A system which makes it possible to increase the intensity through the magnets. A is an earthed electrode in the center of which a small earthed wire C is stretched. B is the electrode on which a negative voltage can be applied.

last section, however, it seems possible to utilize a transmission of 0.5–1 % without considerable time spread.

To still be able to use the experimental set-up with the h.f. deflection plates after the magnets a system to get larger intensity through these without increasing the time spread has been tried. This consists in principle of a focusing unit F which is situated just after the sample but in front of the magnet and with which it is possible to focus into the magnet a larger intensity than was originally possible. Some preliminary measurements with this will be described here.

By the focusing system F one introduces a new source of aberration but the effect of this is in part compensated for by the simultaneous decrease of the aberration of the magnet as the opening angle of this decreases. The same can be said about the magnification of the system. The lens F has a magnification larger than unit, but the magnification of the magnet decreases when F is used. Therefore one could assume that no larger changes of the resolution at the detector will occur.

The time spread in the magnet will decrease by using the arrangement discussed. If one wants a constant value of $d_{r,z}$ (the distance between magnet and image), one must decrease the deflection angle θ_0 of the magnet as the lens F increases the value of d_0. This, in combination with the smaller entrance angle of the magnet, gives a smaller time spread, as can be seen from (10). If one wants to increase the transmission by a factor of 3 for example it is possible to estimate that the time spread is decreased by the same amount.

This qualitative discussion would therefore show that, by using a lens in front

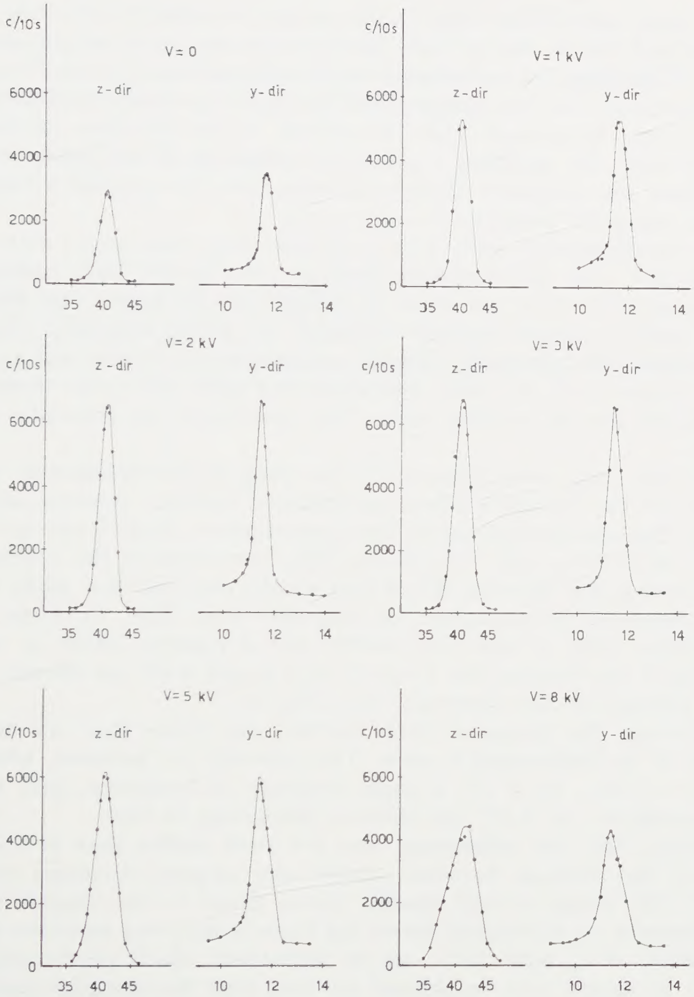

Fig. 9. Radial (y-dir) and axial (z-dir) focusing of electrons of energy 148 keV by use of the system shown in Fig. 8. V represents the negative voltage applied to the electrode B in Fig. 8. The optimum is reached for a value of $V = 3$ kV corresponding to an increase in intensity of about a factor of two. In the z-dir each unit of the abscissa is 4 mm while each unit in the measurement in the y-dir represents a 0.5 mm variation of l, i.e. the distance between the yoke of the magnet and the short-circuiting iron rod (see Fig. 2).

of the magnet, it would be possible to increase the transmission and decrease the time spread without considerable change of the resolution.

What kind of focusing system can be used? As the arrangement has to be small in magnitude, a magnetic field does not seem suitable. An electrostatic system, on the other hand, is usually not possible for higher energies. For low energy, however, a simple three electrode lens system seems applicable. For energies above 50 keV such an arrangement is not practical. Instead, a system shown in Fig. 8 has been tried. This can, under suitable conditions, be used as a focusing system and, as it can be used for energies up to several hundred keV without great difficulties, it is valuable to investigate. In Fig. 8, F consists of a cylindrical electrode B in the center of which a small earthed wire C is stretched. The electrons from the sample pass the system in the direction of the central axis of the cylinder. By applying a negative voltage on B one gets a field inside F, which deflects the electrons, thereby focusing into the magnet a larger intensity than was originally possible.

Preliminary measurements with such a system have been made with electrons of energy 148 keV, the K-conversion electrons of the 239 keV γ-transition in Bi^{212}. The sample S had an extension of about 1.5×1.5 mm^2. The electrode B was situated inside a larger earthed electrode A, which also kept the earthed wire C in position. The electrode B had a diameter of 15 mm and a length of 10 mm. The diameter of the wire was about 0.1 mm. This was therefore also used as a stopper for the central rays. This decreased the intensity by about 10 %.

Fig. 9 gives the shape and intensity of the image at the detector as a function of the voltage on the system F when the distance between detector and magnet was 1.2 m, i.e. the standard distance. The measurement of the focusing was made simultaneously in both z and r directions. The line shape in the z-direction was obtained by moving the detector slit (6 mm width) over the line, while the radial focusing was measured by changing the magnetic field. This, therefore, does not give the absolute value of the line width, but a relative value is, of course, enough. In Fig. 9 the focusing for $V = 0$, 1, 2, 3, 5 and 8 kV are shown. V is here the negative voltage on the electrode B in Fig. 8.

When comparing the shapes of these curves, one notes that up to 3–4 kV on the system F no defocusing is seen. The intensity is, however, increased by about a factor of two. At 5 kV a small decrease of resolution and maximum intensity is measured. At 8 kV an obvious defocusing is seen.

It is surprising that the defocusing does not start earlier than at 5 kV, as the distance d_0, i.e. the distance between sample and magnet, increases when using the system F. The image should thereby move closer to the magnet and cause defocusing. However, as mentioned above the focus is not very sensitive to changes of d_0 (a variation of d_0 with 15 % can be neglected) which partly explains the observed fact. It should also be pointed out here that the electrons passing nearest to the wire in the system F get a larger deflection than those electrons which pass the system at a larger distance from the wire. These should therefore cause a defocusing. That this effect is of less importance must also to a large degree be due to the fact that the focusing is insensitive to small variations of d_0. It must, however, be noticed that the rather large slit width at the detector in the present measurements can partly make small variations in the focusing undetectable.

To reach larger transmission it is necessary to move the detector closer to the magnet. Measurements have been performed at a distance of about 50 cm from the edge of the magnet with the same set up as that described above, but the energy of the electrons was decreased to 55 keV. The reason for using lower energy was that in this case a larger voltage was necessary. When the measurements were made the maximum voltage obtainable was 15 kV, which was not enough for 148 keV electrons. Measurements on 55 keV electrons shows that the intensity of the line increased by about a factor of 2.5 for 15 kV. An arrangement consisting of two focusing systems, one in each channel of the coincidence spectrometer seems therefore to make it possible to increase the coincidence counting rate by about one order of magnitude.

Nobel Institute of Physics, Stockholm 50.

REFERENCES

1. B. Johansson and T. Alväger, Ark. f. Fysik *17*, 163 (1960).
2. N. Svartholm, Ark. f. Fysik *2*, 115 (1950).
3. D. L. Judd, Rev. of Sci. Instr. *21*, 213 (1950).
4. N. Svartholm, Ark. f. Fysik *2*, 195 (1950).
5. P. A. Sturrock, Static and Dynamic electron optics. Cambridge University press (1955).
6. B. Johansson. To be published in Ark. f. Fysik.

Tryckt den 13 april 1960

Uppsala 1960. Almqvist & Wiksells Boktryckeri AB